Spatiotemporal Analysis of Drought and Impact on Millet Production across North Darfur State using Standardized Precipitation Index (SPI) and Reconnaissance Drought Index (RDI)

Mohammed B. Altoom[1, 4,*], Elhadi Adam[1], and Khalid Adem Ali[1, 2], Colbert M. Jackson[1, 3]
[1] Faculty of Science, School of Geography, Archaeology and Environmental Studies, University of the Witwatersrand, Johannesburg 2050, South Africa elhadi.adam@wits.ac.za
[2] Department of Geology and Environmental Geosciences, College of Charleston, Charleston, SC 29424, USA; alika@cofc.edu
[3] Department of Geography, Faculty of Natural and Agricultural Sciences, University of the Free State, Bloemfontein 9300, South Africa; colbermut@gmail.com
[4] Department of Climate & Environment, Faculty of Environmental Sciences &Natural Resources, University of the Al-Fashir, P.O Box 125, Al Fashir, North Darfur State, Sudan.
* Correspondence: 2287659@students.wits.ac.za, mohbasharadam@gmail.com,

DOI: https://dx.doi.org/10.4314/sajg.v13i1.13

Abstract

Drought severely affects the agricultural sector. Its effects have in fact been aggravated by the global warming climate scenario. Although drought has to a large extent been studied globally, it is often overlooked on the local and regional scales. Therefore, accurate and timely characterizations of agricultural drought at the local and regional scales are essential for developing adaptation and mitigation strategies. This study analyzed the spatiotemporal trend of drought events and their impact on millet production in North Darfur State, Sudan from 1981 to 2020. The Standardized Precipitation Index (SPI) and the Reconnaissance Drought Index (RDI) for the three-month (June-August), six-month (June-November), and nine-month (June-February) timescales were used to assess the relevant drought events. The drought-yield relationships were assessed using the Pearson correlation coefficient (r). The results indicate that for detecting drought trends the RDI index is more sensitive to variabilities than the SPI index. The drought events affecting North Darfur over broad spatial extents occurred particularly over the years, 1989, 1990, 1992, 1999, and 2001; the most extreme of drought events being in 2003. The correlation coefficient analysis (r) between the SPI and RDI respectively and the standardized variable of crop yield (SVCY) for millet grain yield showed a strong agreement between the respective variables. The moderate to extreme reductions in millet crop yield occurring in 1992, 1999, 2001, and 2003 corresponded with the moderate to extreme drought indicated by the RDI. Severe crop losses were experienced in Kabkabiya and Umm Kadadda. This study contributes to a clearer understanding of drought impacts on the local scale and thus to insights into developing more effective and targeted management strategies and to enhancing crop resilience.

Keywords: *North Darfur State, drought trends, millet yield, RDI, SPI, standardized variable of crop yield.*

1. Introduction

Drought is one of the most costly and least understood natural disasters (Jiao *et al.*, 2019), significantly impacts the agricultural economy (Yao *et al.*, 2018), and results in the degradation of vegetation and changes in soil properties (Hedo de Santiago *et al.*, 2016, Zarch *et al.*, 2015), thereby impeding long-term socioeconomic growth. Depending on their different impacts, droughts are categorized into four drought types: agricultural, meteorological, hydrological, and socioeconomic droughts (Elhag and Zhang, 2018). Agricultural drought occurs as a result of a soil moisture deficit at a critical time in the growing season, while meteorological drought results from reduced precipitation over an area (Hasan *et al.*, 2019). Hydrological drought arises from a reduction in groundwater and stream flow, and socioeconomic drought refers to the adverse effects of the above types of drought on the lives of the human population (Hasan *et al.*, 2021, Heim Jr, 2002).

Droughts are slow-onset disasters — they have neither a clear beginning nor a definite end — drought is a creeping phenomenon that operates on different time scales and severely impacts economies (Schäfer et al., 2021). Drought causes more damage to agricultural productivity than other common disasters (FAO, 2013; Fawole et al., 2016). Globally, from 1964 to 2007, crop yields issuing from drought declined by about 10% (Lesk *et al.*, 2016). Studying drought is crucial for evaluating agricultural production in countries that heavily rely on rainfed agriculture (Masupha and Moeletsi, 2018). Drought is often studied on a larger scale, thus causing the impacts at the local and regional levels to be neglected (Gjerdi et al., 2019). Therefore, it is important to understand the characteristics and vulnerabilities of local droughts to effectively manage drought (IPCC, 2022, Gjerdi et al., 2019). Most sub-Saharan African countries, including Sudan, are adversely affected by recurrent droughts. Small-scale farming in Sudan is rainfed and, therefore, relies heavily on the levels of soil moisture and fertility (Edreira *et al.*, 2018, Elhag and Zhang, 2018). Sudan suffered from severe droughts during the 20th century, i.e., from 1972 to 1979 and from 1980 to 1984 (Atiem *et al.*, 2022, Teklu *et al.*, 1992). Sudan experienced its worst drought in 1984: it led to a significant drop in crop production, with 4.5 million people suffering from hunger (Elhag and Zhang, 2018, Osman and Shamseldin, 2002). Sudan's Darfur region experiences exacerbated variability/reduction in rainfall, leading to frequent droughts and crop failure (Atiem *et al.*, 2022, Mohmmed *et al.*, 2018).

Several studies have demonstrated that droughts and subsequent land degradation in the Darfur region have led to resource-related conflicts (Dagne, 2009, Faris, 2007, Karamalla-Gaiballa and El-Kafafi, 2021). The Darfur region faces resource-related conflicts emanating from droughts, which have led to desertification and land degradation, thus severely reducing the area of arable land available for the farming and grazing of livestock (Karamalla-Gaiballa and El-Kafafi, 2021). Livestock loss, food shortages, and competition over natural resources have been the natural consequences (Dagne, 2009, Karamalla-Gaiballa and El-Kafafi, 2021). Conflicts have resulted from disputes over land ownership, user rights, and access to grazing areas (Dagne, 2009). Desperate populations resort to theft and looting, escalating social unrest and violence (Dagne, 2009, Faris, 2007, Karamalla-Gaiballa and El-Kafafi, 2021). Therefore, there is a need to evaluate drought impacts on agricultural production and to implement climate adaptation measures in the region (Selby and Hoffmann, 2014).

Previous studies have investigated the spatiotemporal patterns of drought in the world by using meteorological indicators (Abdelmalek and Nouiri, 2020, Atiem *et al.*, 2022, Marini *et al.*, 2019b, Mohmmed *et al.*, 2018, Zarch *et al.*, 2015). Therefore, many indices, such as the Standardized Precipitation Index (SPI), Palmer Drought Severity Index (PDSI), the Standardized Water-level Index (SWI), and the Reconnaissance Drought Index (RDI) are used for studying, evaluating, and monitoring drought. The SPI has been widely used in characterizing drought on various time scales (McKee *et al.*, 1993). The SPI compares the amount of rainfall measured at a given location over several months to the distribution of precipitation over the long term for that period. The PDSI uses precipitation and mean temperature to estimate long-term dryness (Palmer, 1965). Since it lacks long-term continuous soil moisture and actual evapotranspiration data, a PDSI timescale of about nine months makes it possible to detect drought but only inaccurately. Also, the PDSI assumes that all precipitation is rain (Yu *et al.*, 2019). The SWI is computed using both precipitation and potential evapotranspiration -PET (Bhuiyan *et al.*, 2006). To characterize drought, the RDI is calculated using precipitation and temperature data (Tigkas *et al.*, 2016, Zarch *et al.*, 2015).

To determine a suitable drought index is vital to evaluating drought risk (Atiem *et al.*, 2022, Feng *et al.*, 2020). In regions where meteorological stations are scarce or sparsely distributed, the likelihood of droughts is estimated by applying statistical methods and by spatially interpolating spatial data. However, the interpolation process is affected by several factors, leading to extreme uncertainties (Rhee *et al.*, 2010).

Therefore, this study used the SPI and RDI to assess drought events in North Darfur between 1981 and 2020. The RDI is best for spatial studies on a smaller scale, while the SPI is suitable for comparing varying time scales (Merabti *et al.*, 2018). Although there are different indices in use today, the SPI is widely accepted on account of its straightforward structure and because it uses solely precipitation data. Owing to its ability to simulate the intensity of drought in the spatio-temporal dimension, the World Meteorological Organization (WMO) in 2010 made the SPI a key meteorological drought indicator (Svoboda *et al.*, 2012). The temperature variations (minimum and maximum) and the PET used to compute the RDI play a role in determining the response of different crop varieties to drought (Peña-Gallardo *et al.*, 2019). Furthermore, the PET is considered the main factor in agricultural studies (Adnan *et al.*, 2017). The RDI includes the PET because drought severity may emanate from other factors such as changes in temperature, the wind speed, humidity, and PET. The impact of drought on millet crop yield was assessed by examining the correlation between the SPI-3, SPI-6, SPI-9, as well as the RDI-3, RDI-6, and RDI-9 values and the Standardised Variable of Crop Yield (SVCY) from 1998 to 2020. The three six, and nine represent the months of June-August, June-November, and June-February, respectively.

2. Materials and Methods

2.1. Study area

As shown in Figure 1, North Darfur State is situated in western Sudan, between latitudes 11° 45′ 49″ and 20° 00′ 30″ N and between longitudes 22° 46′ 47″ and 27° 29′ 47″ E. The State of North Darfur covers about half the territory of Darfur State. North Darfur is bordered to the northeast by the Northern State, to the east by North Kurdufan, and to the southeast by South Kurdufan. To the south of North Darfur is East Darfur, South Darfur, and Central Darfur, while West Darfur is to the southwest. Also, North Darfur has a common border with Chad and Libya. The state has an area of about 296,420 km^2 and had an estimated population of 2.8 million in 2023. North Darfur has five districts, namely, Umm Kadadda, Kabkabiya, Kutum, Mellit, and AL Fashir (Mohmmed *et al.*, 2018, Young *et al.*, 2005). The Jabbed Marrah Mountains, roughly 3,000 m above sea level, which dominate most of the states of West, Central, and South Darfur, also occupy the southwest of North Darfur State (Osman and Cohen, 2014). The state covers more than 50% of the territory of the Darfur region. Rainfall is slightly higher in the south, and the crops grown include millet, maize, and peanuts. The entire northern region of the state is a desert. The climate is predominantly hot, with long summers (Mohmmed *et al.*, 2018, Siddig, 2010).

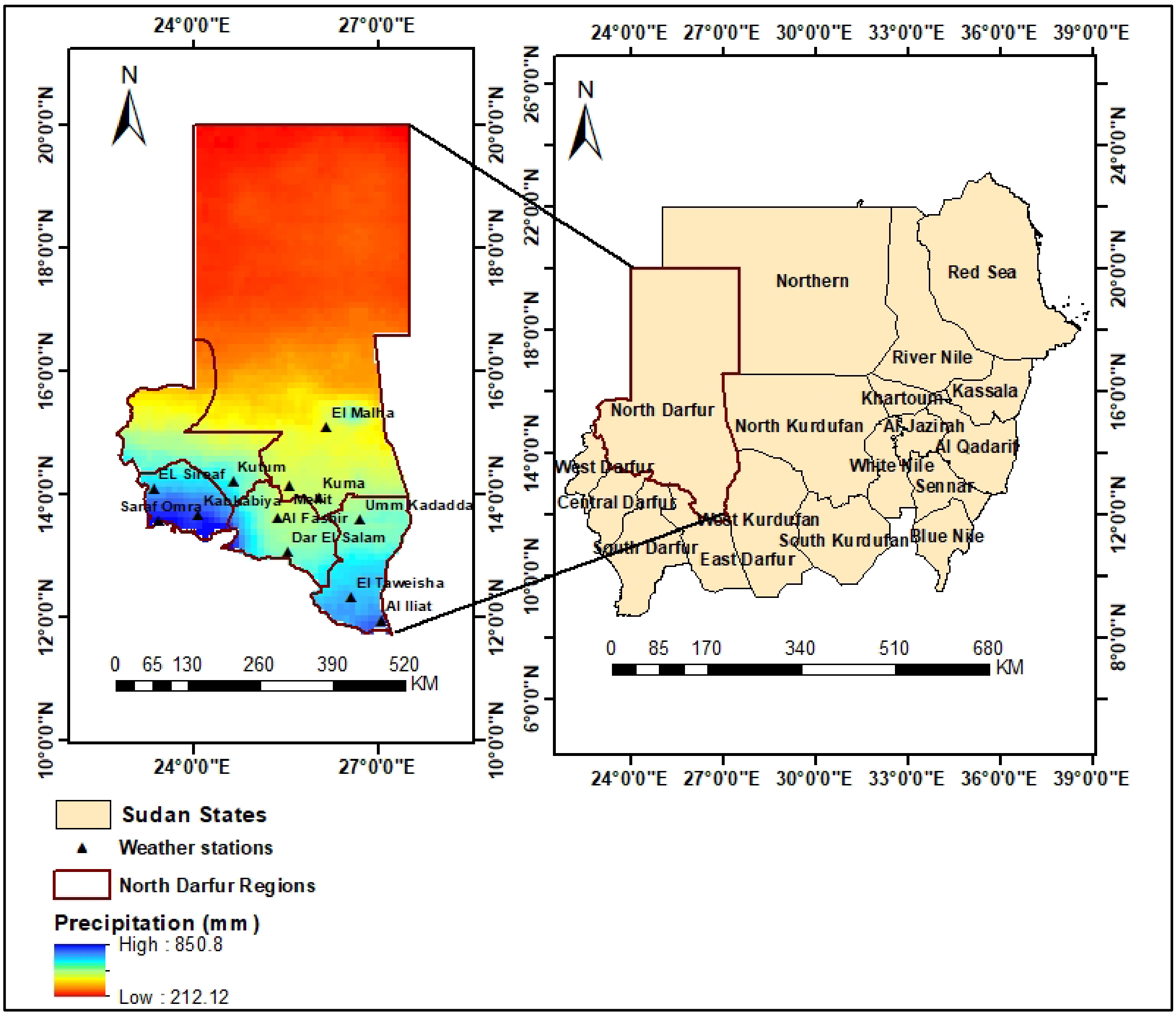

Figure 1. Map of the study area showing the districts and the distribution of meteorological stations in North Darfur State, Sudan.

The distribution of precipitation in the region is characterized by high variability in both temporal and spatial terms. The rainy season extends from June to October, with 70% of the rain falling in July and August. The growth season for millet extends from late June to October. The average annual rainfall in North Darfur ranges from 152 mm in EL Malha in the north to 630 mm in Al Liait in the south. During the summer, temperatures can reach a maximum of 42°C, with some below 11°C in winter (Altoom *et al.*, 2023, Mohmmed *et al.*, 2018).

Rainfed agriculture is the primary livelihood for about 80% of the population in Darfur, and millet, a drought-resistant crop, serves as a major food and cash crop (Siddig, 2010, Young *et al.*, 2005). Agriculture in the south is constrained by the *Goz* sands, which have poor soil fertility (Ibrahim, 1982, Siddig, 2010).

2.2. Data

Meteorological data from 1981 to 2020 from 11 weather stations (Figure 1) distributed across five districts in North Darfur State were obtained from the Ministry of Agriculture. The missing monthly data for all weather stations amounted to less than one percent, and the missing data were interpolated using the inverse distance weighting (IDW) method. Based on the values at the nearby sampled locations, the IDW's estimation of values at the unsampled locations aligns well with the intuitive understanding of how climatic variables vary across space (Abubakar *et al.*, 2020, Elhag and Zhang, 2018). For large-scale applications, the IDW tends to be computationally less demanding while preserving spatial patterns in the data well which are crucial for climatic studies where an understanding of spatial variability and gradients is essential (Harman *et al.*, 2016, Lu and Wong, 2008, Prasetiyowati and Sibaroni, 2018). This preservation of spatial patterns ensures that the interpolated surfaces accurately represent the underlying climatic conditions. Lastly, the IDW's ability to handle non-stationary data without requiring complex statistical assumptions makes it a practical choice for interpolating climatic variables displaying varying spatial patterns (Abubakar *et al.*, 2020, Elhag and Zhang, 2018). Table 1 briefly describes the 11 weather stations used in this study.

The yield data (in tons per ha^{-1} year^{-1}) for the millet crop for the period, 1998 to 2020, for the five districts were also obtained from the Ministry of Agriculture in North Darfur.

Table 1. Characteristics of weather stations in North Darfur State from which meteorological data used in this study were obtained.

ID	Name	Data type	Period	Latitude	Longitude	Elevation masl (m)
1	Al Fashir	Monthly	1981-2020	13° 38'	25° 20'	0740
2	Kutum	Monthly	1981-2020	14° 21'	24° 40'	1160
3	Mellit	Monthly	1981-2020	14° 13'	25° 55'	0900
4	Kabkabiya	Monthly	1981-2020	13° 39'	24° 5'	1120
5	EL Malha	Monthly	1981-2020	15° 09'	26° 15'	0 900
6	Umm Kadadda	Monthly	1981-2020	13° 59'	26° 14'	0595
7	ELTawiesha	Monthly	1981-2020	12° 29'	26° 59'	0591
8	AL Liait	Monthly	1981-2020	11° 57'	27° 04'	0587
9	Saraf Omra	Monthly	1981-2020	13° 47'	23° 30'	1105
10	Kuma	Monthly	1981-2020	13° 39'	26° 01'	0875
11	Dar EL Salam	Monthly	1981-2020	13° 05'	25° 53'	0817

2.3. Methods

The study used the Mann-Kendall test and the Standardized Precipitation Index (SPI) and the Reconnaissance Drought Index (RDI) to analyse drought patterns and trends over the past four decades in North Darfur State. The SPI and RDI could be computed using different monthly time scales, generally from one to 48 months (Eze *et al.*, 2022). The time series of ≤ three months proved to be the most appropriate for the basic monitoring of drought, while ≤ six months could be used to monitor agricultural impacts, and ≥ 12 months was ideal for hydrological impacts (Raziei *et al.*, 2009, Svoboda and Fuchs, 2016). Therefore, the SPI-3

(June-August), SPI-6 (June-November), and SPI-9 (June- February) values — the RDI used the same timescales—were used to assess drought events between 1981 and 2020. The DrinC—Drought Indices Calculator (Lab. of RW & WRM, NTUA, Athens, Greece) software was used to compute the SPI, RDI, and potential evapotranspiration (PET) values — the three displayed relatively small data requirements. As an Excel spreadsheet, the DrinC software was able to calculate drought indices across multiple time scales and to generate outputs (Tigkas *et al.*, 2016).

1.1.1 Standardized Precipitation Index (SPI)

The SPI, by McKee et al. 1993 (McKee *et al.*, 1993) is a widely accepted quantitative measure of drought. The index responds well to dry and/or wet weather conditions (Adhyani *et al.*, 2017). The SPI compares the rainfall amount recorded in a locality for a specific number of months, with the long-term distribution of precipitation for the same number of months (SIRDAŞ and Sen, 2003). However, because the water balance and use are not accounted for, the SPI does not consider the temperature component in detecting droughts (Eze *et al.*, 2022). The index is calculated monthly, with rainfall accumulation periods typically being one, three, six, nine, 12, 24, or 48 months. The corresponding SPIs are denoted as SPI-1, SPI-3, SPI-6, SPI-9, SPI-12, SPI-24, and SPI-48. However, a short period , such as three to six months proved to be preferable for detecting agricultural drought (Raziei *et al.*, 2009). For the purposes of this study, the SPI was focused on SPI-3, SPI-6, and SPI-9, thus corresponding with the precipitation data for the past three, six, and nine months, respectively. The multiple SPIs are very useful for differentiating between the different types of droughts and are thus crucial in quantifying the impacts of a rainfall deficit on water-usable sources. The rainfall data were first applied to calculate the SPI to obtain the estimated gamma parameters. Thereupon, gamma fitting was performed to determine the distribution of the precipitation. The gamma probability density function is defined by Equation 1:

$$g(x) = \frac{1}{\beta^{\alpha}\Gamma(\alpha)} x^{\alpha-1} e^{-\frac{x}{\beta}} \qquad [1]$$

Where x (> 0), β (> 0) and α (> 0) are the precipitation, scale parameter, and shape parameter, respectively.

The SPI values ranged from -3 (dry condition) to +3 (wet condition), and its severity included several classes (McKee et al., 1993, Zhong et al., 2019) (Table 2).

1.1.2 Reconnaissance Drought Index (RDI)

The Reconnaissance Drought Index (RDI) is recommended by the World Meteorological Organization (WMO) as an index for drought characteristics (Hayes *et al.*, 2011). It was also selected for this study because it is highly reliable and broadly accepted by researchers (Vangelis *et al.*, 2013). It is calculated on the basis of rainfall and PET data, which makes it

RDI sensitive to climatic variability. The PET is calculated by applying the following equation (Hargreaves and Samani, 1985):

$$PET = 0.00231 \times Ra \times (Tmean + 17.8) \times TR^{0.5} \quad [2]$$

Where *Ra* is extra-terrestrial radiation, and *TR* is the daily temperature difference between the daily maximum (*Tmax*) and daily minimum (*Tmin*) in °C (*Tmax–Tmin*).

The standardized RDI used in this study was calculated by applying Equation 3:

$$RDI_{(std)}^{(i)} = \frac{y_k^{(i)} - \bar{y}_K}{\sigma_{y_K}} \quad [3]$$

Where y_k,$\bar{y}_k$, and σ_{y_k} are the $ln(\alpha^{(i)}{}_k)$, arithmetic mean of y_k and the standard deviation, respectively.

The values of α_k follow gamma as well as in distributions — but the former proved to be the greatest in diverse study locations and time series (Zarch *et al.*, 2017). Therefore, the gamma probability density function was applied to fit the frequency distribution of α_k (Tsakiris *et al.*, 2008). As opposed to the ordinary conditions of the locality, the RDI positive values indicate the wet period and the negative values the dry period (Table 2).

1.1.3 Drought Trend Analysis

The Mann-Kendall test (Kendall, 1975, Mann, 1945) and Sen's slope (Sen, 1968) were used to analyse the drought trends. Mann Kendall is a non-parametric method widely used to detect trends in climate and hydro-meteorological variables, such as precipitation, temperature, and stream flow. In addition, the Sen method is suitable for estimating the slope of a linear trend. Therefore, the Sen slope determines the magnitude of the change in the climatic variables in the time series models (Lettenmaier *et al.*, 1994). The Mann-Kendall test is based on two hypotheses—null (H_0) expresses no trend, while alternative (H_1) expresses the existence of a linear trend. Using a significant level of five percent if the P value ≤ 0.05, H_1 would be accepted, which means that there is a particular trend in the data. On the other hand, if the *P* value ≥ 0.05, H_0 would be accepted, which would then show no trend in the data. Positive values of *Q* indicate an increasing trend, while negative values indicate a decreasing trend. Values of *Z* that are greater than 1.96 are an indication of a significant increasing trend, whereas *Z* values that are less than -1.96 indicate a significant decreasing trend (Marini *et al.*, 2019a).

This study evaluated drought trends using SPI-3, SPI-6, SPI-9, RDI-3, RDI-6, and RDI-9 for the Umm Kadadda, Kabkabiya, Kutum, Mellit, and AL Fashir districts. In cases where the time series showed a linear trend, the Sen Slope would then be applied to determine its slope and the change rate in the SPI and RDI values.

1.1.4 Crop yield analysis

The most efficient way to assess how droughts affect agriculture is to evaluate agricultural productivity (Foster *et al.*, 2015, Madadgar *et al.*, 2017). Since rain-fed agriculture is majorly practised in the study area, precipitation and PET significantly determine a rise or a decline in crop production. Years of low yields are indicated by negative deviations from normal productivity — thus confirming the existence of drought (Dutta *et al.*, 2015). Therefore, the standardized variable of crop yield (SVCY) was used to assess the effects of drought on agricultural production. The yield-per-hectare data were used to compute the SVCY for all districts in each of the regions within North Darfur (Equation 4):

$$SVCY = \frac{(Y_j - \bar{y})}{\sigma} \qquad [4]$$

The SVCY was used to compute the crop yield loss ratio (YLR) of each district (Equation 5):

$$YLR = \frac{(\bar{y} - Y_j)}{\bar{y}} \times 100\% \qquad [5]$$

Where Y_j,$\bar{y}$, and σ were the crop yields in j year for the state, the long-term average crop yield, and the standard deviation of Y, respectively.

Table 2. Drought and yield classification based on the SPI, RDI, and SVCY values.

SPI/RDI/ values	Drought class	SVCY values	Yield class
≥ 2.0	Extremely wet	1.0 ≥	No yield losses
1.5 to 1.99	Very wet	0 to - 0.49	Normal yield
1.0 to 1.49	Moderately wet	-0.5 to -0.99	Low yield losses
-0.99 to 0.99	Near normal	-1.0 to -1.49	Moderate yield losses
-1.00 to -1.49	Moderately dry	-1.5 to -1.99	Severe yield losses
-1.50 to -1.99	Severely dry	≤ - 2.0	Extreme yield losses
≤ -2.0	Extremely dry		

1.1.5 Relationship between drought and crop yield

To assess the impact of drought on agricultural production in North Darfur, the SVCY was correlated with SPI-3, SPI-6, SPI-9, RDI-3, RDI-6, and RDI-9 in the Umm Kadadda, Kabkabiya, Kutum, Mellit, and AL Fashir districts. The main millet crop areas were Kutum, Kabkabiya, and portions of Al Fashir. The Pearson correlation coefficient (r) was implemented to analyse the relationships. The interpretation of the strength of the associations among the variables was guided by Table 3 and according to the groupings of Cohen *et al.*, 2013.

Table 3. Interpretation of correlation coefficients.

Positive relationship		**Negative relationship**	
Coefficients	Strength	Coefficients	Strength
0.10 to 0.29	Weak	-0.10 to -0.29	Weak
0.30 to 0.49	Moderate	-0.30 to -0.49	Moderate
0.50 to 1.00	Strong	-0.50 to -1.00	Strong

3. Results

3.1. Spatio-temporal distributions of droughts in North Darfur State from 1981 to 2020

The drought analysis shows drought status in negative SPI and RDI values and *vice versa*. The spatial distribution of drought using RDI-3 shows that 1983, 1990, 1992, 1999, and 2001 predominantly experienced moderate drought events; however, 1983, 1990, and 1999 also experienced pockets of severe drought (Figure 2). The SPI-3 reported a moderate drought in 1990, and a relatively small area in Umm Kadadda experienced a severe drought.

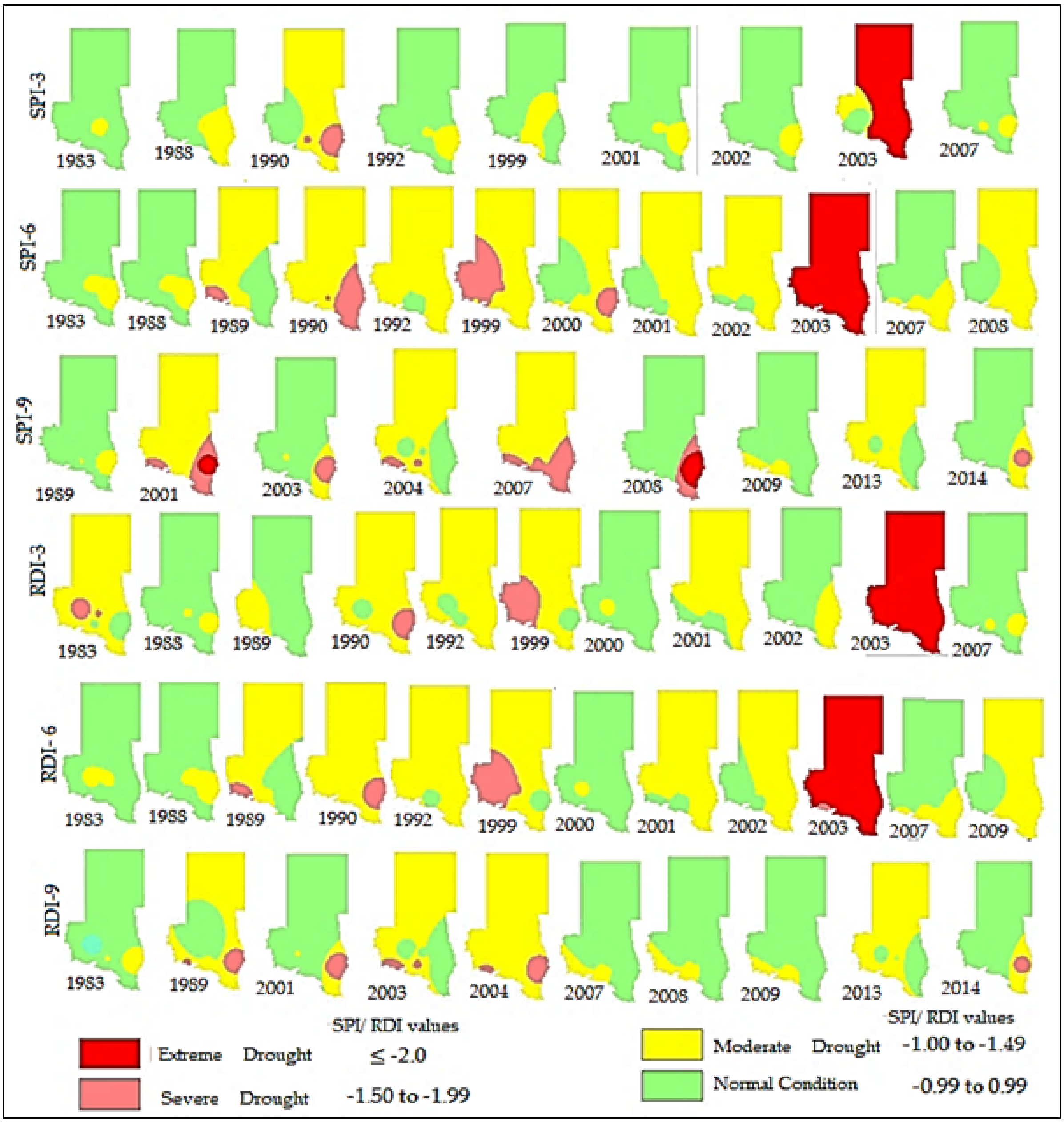

Figure 2. Spatial patterns of drought in North Darfur State from 1981 to 2020 (based on the Standardized Precipitation Index (SPI) and the Reconnaissance Drought Index (RDI)).

Generally, during the study period, the RDI-3 and the SPI-3 showed that only 11 and nine drought events were reported, respectively. Both the SPI-6 and the RDI-6 reported 12 incidents of drought during the study period. The SPI-6 recorded eight events of predominantly moderate drought, i.e., 1989, 1990, 1992, 1999, 2000, 2001, 2002, and 2008, while the RDI-6 reported only seven i.e., 1989, 1990, 1992, 1999, 2001, 2002, and 2009. Still, both indices recorded severe drought in parts of Kabkabiya in 1989, Umm Kaddada in 1990, and Kutum and Kabkabiya in 1999. The SPI-9 reported moderate droughts in 2001, 2004, 2007, and 2013, while the RDI-9's were in 1989, 2003, 2004, and 2013. Both indices and their respective months recorded events of extreme drought in 2003. Overall, the RDI index detected more years of drought than the SPI index. In 2003, the extreme drought experienced in North Darfur was more intense in the Kutum and Mellit districts (Figure 3). Generally, more drought events were experienced in Al Fashir, Kabkabiya, and Umm Kadadda than in the Kutum and Mellit districts.

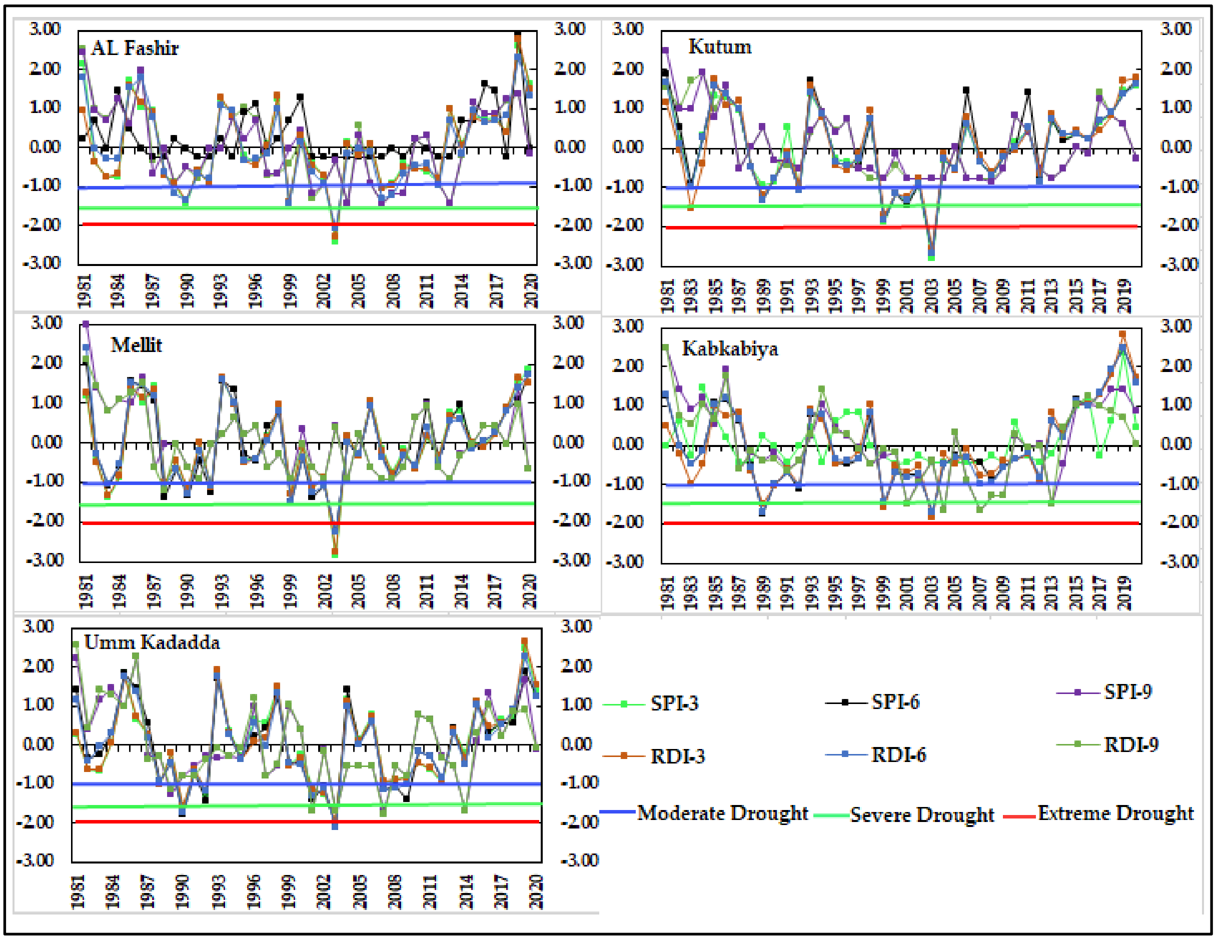

Figure 3. Standardized Precipitation and Reconnaissance Drought Indices values in North Darfur State on three timescales (three months, six months, nine months and from 1981-2020).

3.2. Trend analysis of drought in North Darfur

The Mann-Kendall test and Sen's slope estimator results are summarized in Table 4 and show that drought trends were not significant at five percent in the five districts of North Darfur State. A positive trend indicates increased precipitation and *vice versa*. The SPI and the RDI trends (Kendall Tau-b) ranged from 0.262 to -0.255 (Table 4). The Sen's slope ranged from 0.028 to -0.022. The correlation of the SPI and the RDI trends (Kendall Tau-b) for the three-month timescale for the SPI and the RDI showed positive trends for all five districts. The same applies to the six-month timescale for all districts, except Kutum, which had a -0.233 for the SPI, symbolising rising drought intensity. The nine month timescale for the SPI showed a positive trend for all districts, while the RDI showed a negative trend—therefore, the RDI pointed out an increasing drought intensity in all five districts. Numbered lists can be added as follows:

Table 4. The statistical trend test results for different timescales for the SPI and the RDI of the five districts over the period 1981-2020.

District	MK (Z)			*P*-Value[a]-months			Sen's Slope Estimate (Q)		
	SPI-3	SPI-6	SPI-9	SPI-3	SPI-6	SPI-9	SPI-3	SPI-6	SPI-9
Al Fashir	0.103	0.114	0.023	0.009	0.038	0.017	0.018	0.000	0.006
Kutum	0.146	-0.233	0.074	0.106	0.087	0.023	0.000	0.018	0.012
Mellit	0.152	0.168	0.082	0.118	0.101	0.022	0.021	0.017	0.012
Kabkabiya	0.262	0.006	0.131	0.151	0.139	0.028	0.000	0.019	0.022
Umm Kadadda	0.121	0.125	0.062	0.060	0.073	0.016	0.016	0.008	0.010
	RDI-3	RDI-6	RDI-9	RDI-3	RDI-6	RDI-9	RDI-3	RDI-6	RDI-9
Al Fashir	0.103	0.049	-0.130	0.357	0.666	0.244	0.017	0.008	-0.021
Kutum	0.146	0.100	-0.255	0.188	0.370	0.024	0.023	0.017	-0.022
Mellit	0.172	0.113	-0.243	0.121	0.311	0.030	0.022	0.016	-0.022
Kabkabiya	0.262	0.154	-0.135	0.018	0.166	0.226	0.028	0.020	-0.019
Umm Kadadda	0.121	0.049	-0.136	0.279	0.666	0.221	0.016	0.007	-0.012

3.3. Impact of drought on millet production

The variability in the spatial occurrence and severity of droughts also led to variability in the millet crop yield in the five districts of North Darfur – in fact, to a decline. Based on the threshold values listed in Table.2, extreme crop losses, SVCY ≤ - 2.0, were not recorded in any district during the study period, while severe crop losses, -1.5 <SVCY> -1.99, were recorded in the Al Fashir, Kabkabiya, and Umm Kadadda districts in 2003. Furthermore, moderate crop losses, -1.0 <SVCY>-1.49, were recorded in Kabkabiya and Umm Kadadda in 2000, 2001, 2003, 2004, 2005, 2007, 2009, and 2015. As shown in Figure 4, ll districts recorded low crop losses, -0.5 <SVCY> -0.99. By comparing the SPI and the RDI for the respective timescales for the five districts in North Darfur, overall, their values showed a positive relationship with crop yield, i.e., an increase in the indices resulted in a rise in crop yield and *vice versa*.

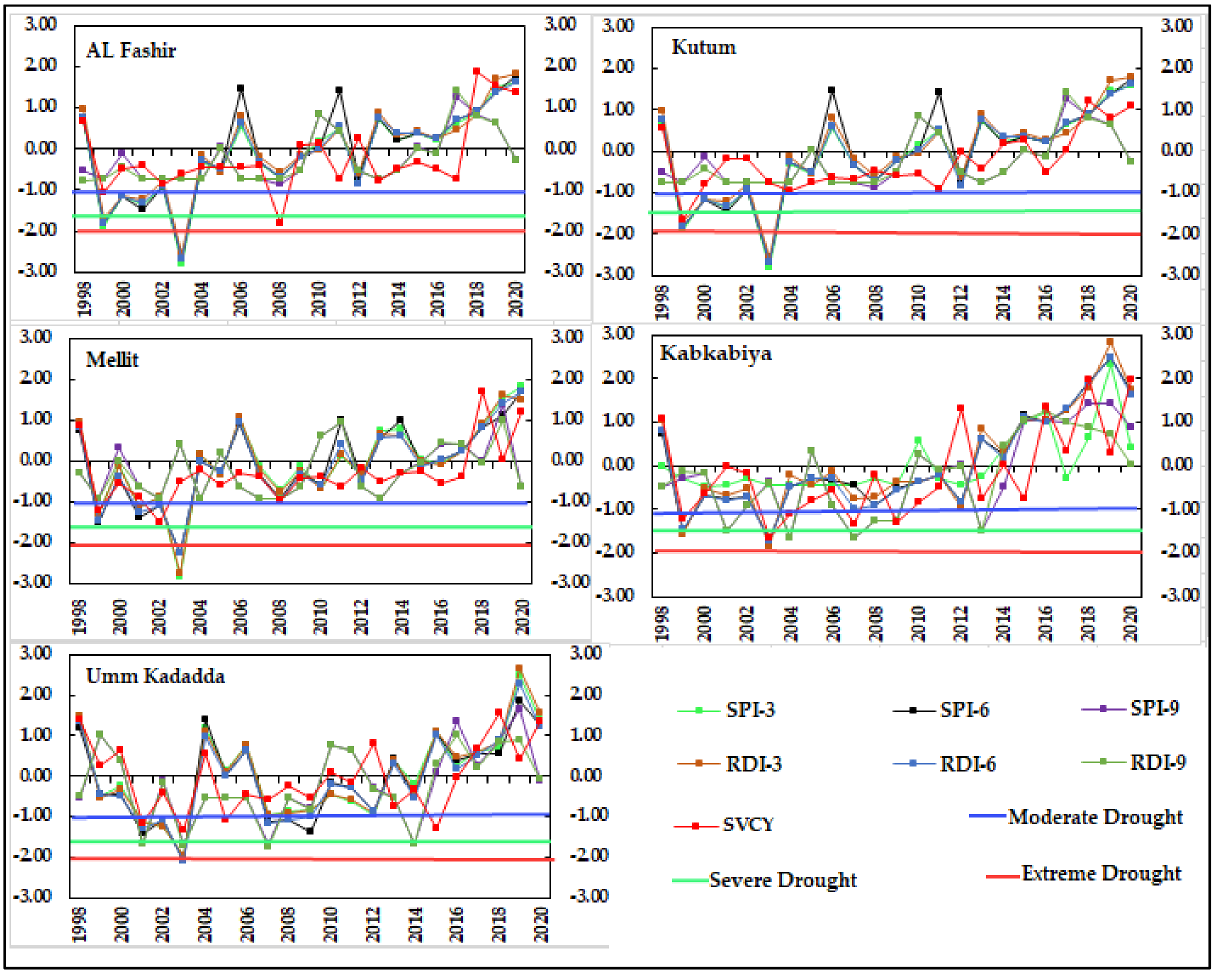

Figure 4. Drought and crop yield analysis of Umkadada, Kabkabiya, Kutum, Mellit, and Al Fasher districts, North Darfur, from 1998-2020.

Table 5 shows the statistical relationship between drought trend and SVCY using the SPI and the RDI as determined by applying the Pearson correlation coefficient (r). The results depict a moderate to strong relationship between SVCY and drought for the indices for all the timescales used in the study for all districts, with the exception of Mellit (SPI- and RDI-9), which showed a weak relationship. In general, the results show that droughts impacted millet yield in North Darfur State.

Table 5. Statistical relationship between drought trend and SVCY using the SPI and the RDI.

SVCY/Indices	SPI-3	SPI-6	SPI-9	RDI-3	RDI-6	RDI-9
Al Fashir	0.57	0.50	0.43	0.58	0.55	0.38
Kutum	0.65	0.55	0.38	0.66	0.65	0.36
Mellit	0.63	0.64	0.14	0.63	0.68	0.15
Kabkabiya	0.40	0.63	0.55	0.62	0.65	0.47
Umm Kadadda	0.49	0.51	0.50	0.48	0.51	0.48

4. Discussion

By using the Standardized Precipitation Index (SPI) and the Reconnaissance Drought Index (RDI), this study conducted a spatiotemporal analysis of drought and how drought affected millet yield in North Darfur over the study period. The nonparametric Mann-Kendall test and Sen's slope approach were used to investigate the long-term trend of droughts in the study area. The Pearson correlation (*r*) was used to analyse the relationship between drought and millet crop yield.

Rainfall and minimum and maximum temperatures over about 40 years were used to calculate the drought indices, i.e., the SPI and the RDI, used to detect drought in the study area. The indices were calculated at varying timescales (3, 6, and 9 months) between 1981 and 2020. Only drought events were examined even though the SPI and RDI time series included both drought and non-drought statuses. The main periods of drought according to the SPI were 1989, 1990, 1992, 1999, 2000, 2001, 2002, 2004, 2003, 2007, 2008, and 2013. The RDI reported droughts in 1983, 1989, 1990, 1992, 1999, 2000, 2001, 2002, 2004, 2003, 2009, and 2013 (Figure 2). These findings align with previous studies such as those undertaken by Elhag and Zhang (2018) and Mohamed *et al*. (2018), respectively. The analysis showed normal conditions and drought status with positive and negative SPI and RDI values — the positive values indicating wetness and the negative values related to dryness (Figure 3). This analysis shows that drought is a frequent phenomenon in the study area. Even though the SPI and RDI values showed that the intensity and frequency of drought tended to fade in certain years; they variables would then recur within the next few years. Differences were also evident between the SPI and the RDI for the respective timescales. The spatial analysis showed the variability of the drought patterns across the state over the years. Parts of the Umm Kadadda and Kabkabiya districts were the most severely affected by drought: — some places in these two districts were even experiencing drought when normal conditions were prevailing in other parts of North Darfur, (e.g., RDI-3 (1989), SPI-3 (1992), and SPI-6 (2007)). When other places were experiencing moderate drought conditions, parts of the Umm Kadadda and Kabkabiya districts would still be experiencing severe drought (e.g., RDI-3 (1999) and SPI-6 (1999)). Drought trends over the short term, i.e., based on three-month periods for SPI and RDI, showed that North Darfur State was affected by extreme, severe, and moderate drought conditions, respectively. Short-term drought events proved to be linked to the El Nino/Southern Oscillation (ENSO) (Elhag and Zhang, 2018). This study found that the RDI index is more sensitive to variabilities than the SPI index when it comes to detecting drought trends. For example, the SPI index results showed that 1999 and 2003 in the Kabkabiya and Al Fashir districts favoured normal conditions. Nevertheless, compared to the RDI values, the results showed that the Kabkabiya and Al Fashir districts were experiencing severe to extreme droughts. This sensitivity is due to the effect of the temperature element in the PET used in calculating he RDI (Peña-Gallardo *et al.*, 2019). This consideration is consistent with the findings of several studies worldwide that reported that PET is considered the main factor in agricultural studies (Abdelmalek and Nouiri, 2020, Abubakar *et al.*, 2020, Adnan *et al.*, 2017).

Droughts have persisted in North Darfur and threaten agricultural productivity (Mohmmed *et al.*, 2018). The results of the impact of drought on millet crop yields show that droughts generally lead to decreased production in North Darfur State. Severe crop losses occurred in Umm Kadadda, Al Fashir, and Kabkabiya in 2003. Moderate losses in crop yield were experienced in Umm Kadadda and Kabkabiya in 2000, 2001, 2003, 2004, 2005, 2007, 2009, and 2015. As shown in Figure 4, the five districts of North Darfur recorded low crop losses during the study period. These results agree with the findings of a study conducted in Sudan by Elhag and Zhang (2018) (Elhag and Zhang, 2018). According to Liu et al. (2018) (Liu *et al.*, 2018), short to medium-term droughts could impact millet yields in North Darfur State. Overall, the correlation analysis between drought and the standardized variable of crop yield (SVCY) shows a moderate to strong relationship between these two variables for the SPI and the RDI for all timescales. The SPI and the RDI values showed positive relationships with crop yield—a decline in the indices' values resulted in a decline in the crop yield, while an increase in the SPI and RDI values meant an increase in the crop yield (Figure 4). Therefore, this highlights the role that drought plays in controlling the vulnerability of agricultural communities in the study area—it makes North Darfur State susceptible to droughts and climate change.

The North Darfur State experiences extreme temperatures, fluctuating rainfall, and drought. The unreliable rainfall, combined with drought, makes North Darfur highly vulnerable to the slightest decrease in rainfall or a temperature rise (Cheeseman, 2016). The temperature increases have resulted in a decline in precipitation. Indeed, under its current climate, North Darfur is faced with recurrent food insecurity and water scarcity, declining soil fertility, and the absence of a sound physical security system, triggered and/or exacerbated by climate variability, all of which alter agricultural productivity (Twongyirwe *et al.*, 2019). Therefore, drought, the main factor determining crop yields — as manifested in the low soil moisture content and the high PET losses − tends to reduce crop productivity. Furthermore, low precipitation has contributed to the increased drought conditions in the study area and has severely affected the rainfed agricultural system mainly practised in North Darfur (Mohmmed *et al.*, 2018). If no significant adaptations are made, climate change will put the livelihoods of those living in the larger part of the study area at increased risk of drought. Thus, farmers should use techniques that minimize soil moisture loss and be informed about preferable planting dates in each new season. Also, should the weather forecasting systems indicate an unreliable rainfall year, farmers should implement appropriate measures. Owing to its high exposure and sensitivity to unfavourable climatic conditions, North Darfur is extremely vulnerable to drought impacts (Mohmmed *et al.*, 2018). Natural meteorological conditions, as well as the low level of socioeconomic development in the study area, have contributed to this specific vulnerability (Noureldeen *et al.*, 2020). Aggravating droughts and related hazards are expected to increase across North Darfur (Arias *et al.*, 2021, Gizaw and Gan, 2017). The drought trend analysis showed that the RDI has indicated an increasing drought intensity over the last 40 years in all five districts of North Darfur. As much as adaptations to climate change are implemented in a timely and effective way, controlling population growth could prove to be a better measure to mitigate drought risk; this can be attributed to the improvement that it brings in socioeconomic vulnerability, which can in fact reduce potential exposure to drought (Mohmmed *et al.*, 2018).

5. Conclusions

Climate change has led to more intense local and regional droughts and their related impacts—North Darfur is no exception. Quantifying and understanding drought occurrence and its consequences for agricultural production and ecosystems is particularly important. This study carried out a spatio-temporal analysis of drought and the effect of drought on rainfed millet crop production in North Darfur State in Sudan. It used the Standardized Precipitation Index (SPI) and the Reconnaissance Drought Index (RDI), and the standardized variable of crop yield (SVCY). Climate change has significantly threatened human well-being and food security in North Darfur. Generally, the results of this study will provide decision-makers with a better understanding of the spatio-temporal evolution of drought in North Darfur State to help mitigate the devastating impact of drought. Therefore, future development programs on the local and international level that concentrate on adaptations to climate change and the mitigation of its effects could benefit by being based on these results and by targeting even the most vulnerable agricultural areas. This study proposes improvements to those regions experiencing severe drought conditions that have been mapped by comprehensively comparing different spatial estimation approaches, and in so doing, develop an efficient drought-monitoring system.

6. Acknowledgements

We wish to acknowledge the role of the Ministry of Agriculture in providing the data on the climate and millet yields for North Darfur State.

7. References

Abdelmalek, M. B. & Nouiri, I. 2020. Study of trends and mapping of drought events in Tunisia and their impacts on agricultural production. *Science of the Total Environment,* 734, 139311.

Abubakar, H. B.; Newete, S. W. & Scholes, M. C. 2020. Drought characterization and trend detection using the reconnaissance drought index for Setsoto Municipality of the Free State Province of South Africa and the impact on maize yield. *Water,* 12, 2993.

Adhyani, N.; June, T. & Sopaheluwakan, A. Exposure to drought: Duration, severity and intensity (Java, Bali and Nusa Tenggara). IOP Conference Series: Earth and Environmental Science, 2017. IOP Publishing, 012040.

Adnan, S.; Ullah, K.; Khan, A. H. & Gao, S. 2017. Meteorological impacts on evapotranspiration in different climatic zones of Pakistan. *Journal of Arid Land,* 9, 938-952.

Altoom, M. B.; Adam, E. & Ali, K. A. 2023. Mapping and Monitoring Spatio-temporal Patterns of Rainfed Agriculture Lands of North Darfur State, Sudan, using Earth Observation Data. *Land,* 12, 307.

Arias, P.; Bellouin, N.; Coppola, E.; Jones, R.; Krinner, G.; Marotzke, J.; Naik, V.; Palmer, M.; Plattner, G.-K. & Rogelj, J. 2021. Climate Change 2021: the physical science basis. Contribution of Working Group I to the Sixth Assessment Report of the Intergovernmental Panel on Climate Change; technical summary.

Atiem, I. A.; Siddig, M. S.; Hamukwaya, S. L.; Ahmed, H. I.; Taha, M. M.; Ibrahim, S. & Osman, Y. 2022. Assessment of seasonal rainfall drought indices, Nyala City Sudan. *Agriculture,* 12, 1069.

Bhuiyan, C.; Singh, R. & Kogan, F. 2006. Monitoring drought dynamics in the Aravalli region (India) using different indices based on ground and remote sensing data. *International Journal of Applied Earth Observation and Geoinformation,* 8, 289-302.

Cheeseman, J. 2016. Food security in the face of salinity, drought, climate change, and population growth. *Halophytes for food security in dry lands.* Elsevier.

Cohen, J.; Cohen, P.; West, S. G. & Aiken, L. S. 2013. *Applied multiple regression/correlation analysis for the behavioral sciences*, Routledge.

Dagne, T. S. 2009. *Sudan: The crisis in Darfur and the status of the North-South Peace Agreement*, Congressional Research Service.

Dutta, D.; Kundu, A.; Patel, N.; Saha, S. & Siddiqui, A. 2015. Assessment of agricultural drought in Rajasthan (India) using the Remote Sensing-derived Vegetation Condition Index (VCI) and the Standardized Precipitation Index (SPI). *The Egyptian Journal of Remote Sensing and Space Science,* 18, 53-63.

Edreira, J. I. R.; Guilpart, N.; Sadras, V.; Cassman, K. G.; van Ittersum, M. K.; Schils, R. L. & Grassini, P. 2018. Water productivity of rainfed maize and wheat: A local to global perspective. *Agricultural and Forest Meteorology,* 259, 364-373.

Elhag, K. M. & Zhang, W. 2018. Monitoring and assessment of drought focused on its impact on sorghum yield over Sudan by using meteorological drought indices for the period 2001–2011. *Remote Sensing,* 10, 1231.

Eze, E.; Girma, A.; Zenebe, A.; Okolo, C. C.; Kourouma, J. M. & Negash, E. 2022. Predictors of drought-induced crop yield/losses in two agroecologies of southern Tigray, Northern Ethiopia. *Scientific Reports,* 12, 6284.

Faris, S. 2007. The real roots of Darfur. *Atlantic Monthly,* 299, 67.

Feng, K.; Su, X.; Zhang, G.; Javed, T. & Zhang, Z. 2020. Development of a new integrated hydrological drought index (SRGI) and its application in the Heihe River Basin, China. *Theoretical and Applied Climatology,* 141, 43-59.

Food and Agriculture Organization of the United Nations (FAO). UN lays Foundations for more Drought Resilient Societies. Meeting urges Disaster-risk Reduction instead of Crisis Management; FAO: Roma, Italy, 2013. 3.

Fawole, W.O.; Ozkan, B.; Ayanrinde, F.A. Measuring food security status among households in Osun State, Nigeria. British Food Journal. 2016, 118, 1554–1567

Foster, T.; Brozović, N. & Butler, A. 2015. Why well yield matters for managing agricultural drought risk. *Weather and Climate Extremes,* 10, 11-19.

Gizaw, M. S. & Gan, T. Y. 2017. Impact of climate change and El Niño episodes on droughts in sub-Saharan Africa. *Climate Dynamics,* 49, 665-682.

Gjerdi, H. L.; Gunn, T.; Mishra, A.; Pulwarty, R. S. & Sheffield, J. 2019. Droughts in the Anthropocene / Sequías en el Antropoceno. UNESCO and GRID-Arendal.

Hargreaves, G. H. & Samani, Z. A. 1985. Reference crop evapotranspiration from temperature. *Applied ERngineering in Agriculture,* 1, 96-99.

Harman, B. I.; Koseoglu, H. & Yigit, C. O. 2016. Performance evaluation of IDW, Kriging and multiquadric interpolation methods in producing noise mapping: A case study at the city of Isparta, Turkey. *Applied Acoustics,* 112, 147-157.

Hasan, H. H.; Mohd Razali, S. F.; Muhammad, N. S. & Ahmad, A. 2019. Research trends of hydrological drought: A systematic review. *Water,* 11, 2252.

Hasan, H. H.; Mohd Razali, S. F.; Muhammad, N. S. & Mohamad Hamzah, F. 2021. Assessment of probability distributions and analysis of the minimum storage draft rate in the equatorial region. *Natural Hazards and Earth System Sciences,* 21, 1-19.

Hayes, M.; Svoboda, M.; Wall, N. & Widhalm, M. 2011. The Lincoln declaration on drought indices: universal meteorological drought index recommended. *Bulletin of the American Meteorological Society,* 92, 485-488.

Hedo de Santiago, J.; Lucas-Borja, M. E.; Wic-Baena, C.; Andrés-Abellán, M. & de las Heras, J. 2016. Effects of thinning and induced drought on microbiological soil properties and plant species diversity at dry and semiarid locations. *Land Degradation & Development,* 27, 1151-1162.

Heim Jr, R. R. 2002. A review of twentieth-century drought indices used in the United States. *Bulletin of the American Meteorological Society,* 83, 1149-1166.

Ibrahim, F. N. 1982. The role of women peasants in the process of desertification in Western Sudan. *GeoJournal,* 6, 25-30.

IPCC (Intergovernmental Panel on Climate Change), 2022: Summary for Policymakers [H.-O. Pörtner, D.C. Roberts, E.S. Poloczanska, K. Mintenbeck, M. Tignor, A. Alegría, M. Craig, S. Langsdorf, S. Löschke, V. Möller, A. Okem (eds.)]. In: Climate Change 2022: Impacts, Adaptation and Vulnerability. Contribution of Working Group II to the Sixth Assessment Report of the Intergovernmental Panel on Climate Change [H.-O. Pörtner, D.C. Roberts, M. Tignor, E.S. Poloczanska, K. Mintenbeck, A. Alegría, M. Craig, S. Langsdorf, S. Löschke, V. Möller, A. Okem, B. Rama (eds.)]. Cambridge University Press, Cambridge, UK and New York, NY, USA, pp. 3–33.

Jiao, W.; Tian, C.; Chang, Q.; Novick, K. A. & Wang, L. 2019. A new multi-sensor integrated index for drought monitoring. *Agricultural and Forest Meteorology,* 268, 74-85.

Karamalla-Gaiballa, N. & El-Kafafi, S. 2021. The Impact of Conflicts on Natural Resources – The Case of the Sudanese Darfur Region. *Polish Political Science Yearbook,* 50, 1-12.

Kendall, M. 1975. Rank Correlation Methods, Charles Griffin, London (1975). *Google Scholar*.

Lesk, C.; Rowhani, P. & Ramankutty, N. 2016. Influence of extreme weather disasters on global crop production. *Nature,* 529, 84-87.

Lettenmaier, D. P.; Wood, E. F. & Wallis, J. R. 1994. Hydro-climatological trends in the continental United States, 1948-88. *Journal of Climate,* 7, 586-607.

Liu, X.; Pan, Y.; Zhu, X.; Yang, T.; Bai, J. & Sun, Z. 2018. Drought evolution and its impact on the crop yield in the North China Plain. *Journal of Hydrology,* 564, 984-996.

Lu, G. Y. & Wong, D. W. 2008. An adaptive inverse-distance weighting spatial interpolation technique. *Computers & Geosciences,* 34, 1044-1055.

Madadgar, S.; AghaKouchak, A.; Farahmand, A. & Davis, S. J. 2017. Probabilistic estimates of drought impacts on agricultural production. *Geophysical Research Letters,* 44, 7799-7807.

Mann, H. B. 1945. Nonparametric tests against trend. *Econometrica: Journal of the Econometric Society*, 245-259.

Marini, G.; Fontana, N. & Mishra, A. K. 2019a. Investigating drought in the Apulia region, Italy, using SPI and RDI. *Theoretical and Applied Climatology,* 137, 383-397.

Marini, G.; Fontana, N. & Mishra, A. K. 2019b. Investigating drought in the Apulia region, Italy, using SPI and RDI. *Theoretical and Applied Climatology,* 137, 383-397.

Masupha, T. E. & Moeletsi, M. E. 2018. Analysis of potential future droughts limiting maize production in the Luvuvhu River catchment area, South Africa. *Physics and Chemistry of the Earth, Parts A/B/C,* 105, 44-51.

McKee, T. B.; Doesken, N. J. & Kleist, J. The relationship of drought frequency and duration to time scales. Proceedings of the Eighth Conference on Applied Climatology, 1993. California, 179-183.

Merabti, A.; Meddi, M.; Martins, D. S. & Pereira, L. S. 2018. Comparing SPI and RDI applied at local scale as influenced by climate. *Water Resources M<anagement,* 32, 1071-1085.

Mohmmed, A.; Zhang, K.; Kabenge, M.; Keesstra, S.; Cerdà, A.; Reuben, M.; Elbashier, M. M.; Dalson, T. & Ali, A. A. 2018. Analysis of drought and vulnerability in the North Darfur region of Sudan. *Land Degradation & Development,* 29, 4424-4438.

Noureldeen, N.; Mao, K.; Mohmmed, A.; Yuan, Z. & Yang, Y. 2020. Spatiotemporal drought assessment over Sahelian countries from 1985 to 2015. *Journal of Meteorological Research,* 34, 760-774.

Osman, A. M. K. & Cohen, M. J. 2014. We no longer share the Land: Agricultural change, land, and violence in Darfur.

Osman, Y. Z. & Shamseldin, A. Y. 2002. Qualitative rainfall prediction models for central and southern Sudan using El Niño–Southern Oscillation and Indian Ocean sea surface temperature indices. *International Journal of Climatology* , 22, 1861-1878.

Palmer, W. 1965. Meteorological drought. US Weather Bureau Research Paper 45, 58 pp.

Peña-Gallardo, M.; Vicente-Serrano, S. M.; Quiring, S.; Svoboda, M.; Hannaford, J.; Tomas-Burguera, M.; Martín-Hernández, N.; Domínguez-Castro, F. & El Kenawy, A. 2019. Response of crop yield to different time-scales of drought in the United States: Spatio-temporal patterns and climatic and environmental drivers. *Agricultural and Forest Meteorology,* 264, 40-55.

Prasetiyowati, S. & Sibaroni, Y. Prediction of DHF disease spreading patterns using inverse distances weighted (IDW), ordinary and universal kriging. Journal of Physics: Conference Series, 2018. IOP Publishing, 012010.

Raziei, T.; Saghafian, B.; Paulo, A. A.; Pereira, L. S. & Bordi, I. 2009. Spatial patterns and temporal variability of drought in western Iran. *Water Resources Management,* 23, 439-455.

Rhee, J.; Im, J. & Carbone, G. J. 2010. Monitoring agricultural drought for arid and humid regions using multi-sensor remote sensing data. *Remote Sensing of the Environment,* 114, 2875-2887.

Schäfer, L.; Jorks, P.; Seck, E.; Koulibaly, O.; Diouf, A. 2021. Slow-onset processes and resulting loss and damage - an introduction.

Selby, J. & Hoffmann, C. 2014. Beyond scarcity: rethinking water, climate change and conflict in the Sudans. *Global Environmental Change,* 29, 360-370.

Sen, P. K. 1968. Estimates of the regression coefficient based on Kendall's tau. *Journal of the American Statistical Association,* 63, 1379-1389.

Siddig, K. 2010. Macroeconomy and agriculture in Sudan: Analysis of trade policies, external shocks, and economic bans in a computable general equilibrium approach. Available at SSRN 1684084.

SIRDAŞ, S. & Sen, Z. 2003. Spatio-temporal drought analysis in the Trakya region, Turkey. *Hydrological Sciences Journal,* 48, 809-820.

Svoboda, M. & Fuchs, B. 2016. Handbook of drought indicators and indices. *Drought and Water Crises: Integrating Science, Management, and Policy*, 155-208.

Svoboda, M.; Hayes, M. & Wood, D. 2012. Standardized precipitation index: user guide.

Teklu, T.; Von Braun, J. & Zaki, E. 1992. Drought and famine relationships in Sudan: Policy implications. *Food and Nutrition Bulletin,* 14, 1-3.

Tigkas, D.; Vangelis, H. & Tsakiris, G. 2016. Introducing a modified reconnaissance drought index (RDI) incorporating effective precipitation. *Procedia Engineering,* 162, 332-339.

Tsakiris, G.; Nalbantis, I.; Pangalou, D.; Tigkas, D. & Vangelis, H. Drought meteorological monitoring network design for the reconnaissance drought index (RDI). Proceedings of the first International Conference on "Drought management: scientific and technological innovations". Zaragoza, Spain: Option Méditerranéennes, Series A, 2008. Citeseer, 2008.

Twongyirwe, R.; Mfitumukiza, D.; Barasa, B.; Naggayi, B. R.; Odongo, H.; Nyakato, V. & Mutoni, G. 2019. Perceived effects of drought on household food security in South-western Uganda: Coping responses and determinants. *Weather and Climate Extremes,* 24, 100201.

Vangelis, H.; Tigkas, D. & Tsakiris, G. 2013. The effect of PET method on Reconnaissance Drought Index (RDI) calculation. *Journal of Arid Environments,* 88, 130-140.

Yao, N.; Li, Y.; Lei, T. & Peng, L. 2018. Drought evolution, severity and trends in Mainland China over 1961–2013. *Science of the Total Environment,* 616, 73-89.

Young, H.; Osman, A. M.; Aklilu, Y.; Dale, R.; Badri, B. & Fuddle, A. 2005. Darfur 2005 Livelihoods under Siege. *Medford: Feinstien International Famine Center, Tufts University*, 130.

Yu, H.; Zhang, Q.; Xu, C.-Y.; Du, J.; Sun, P. & Hu, P. 2019. Modified palmer drought severity index: model improvement and application. *Environment International,* 130, 104951.

Zarch, M. A. A.; Sivakumar, B.; Malekinezhad, H. & Sharma, A. 2017. Future aridity under conditions of global climate change. *Journal of Hydrology,* 554, 451-469.

Zarch, M. A. A.; Sivakumar, B. & Sharma, A. 2015. Droughts in a warming climate: A global assessment of the Standardized Precipitation Index (SPI) and the Reconnaissance Drought Index (RDI). *Journal of Hydrology,* 526, 183-195.

Zhong, R.; Chen, X.; Lai, C.; Wang, Z.; Lian, Y.; Yu, H. & Wu, X. 2019. Drought monitoring utility of satellite-based precipitation products across Mainland China. *Journal of Hydrology,* 568, 343-359.